

Article

# Cr Release from Cr-Substituted Goethite during Aqueous Fe(II)-Induced Recrystallization

Jian Hua <sup>1,2,3,†</sup>, Manjia Chen <sup>2,†</sup>, Chengshuai Liu <sup>1,\*</sup>, Fangbai Li <sup>2</sup>, Jian Long <sup>3</sup>, Ting Gao <sup>1,2</sup>, Fei Wu <sup>1,2</sup>, Jing Lei <sup>4</sup> and Minghua Gu <sup>4</sup>

<sup>1</sup> State Key Laboratory of Environmental Geochemistry, Institute of Geochemistry, Chinese Academy of Sciences, Guiyang 550081, China; huajiany1211@163.com (J.H.); gaoting\_gt0@163.com (T.G.); wufei@soil.gd.cn (F.W.)

<sup>2</sup> Guangdong Key Laboratory of Integrated Agro-Environmental Pollution Control and Management, Guangdong Institute of Eco-Environmental Science & Technology, Guangzhou 510650, China; mjchen@soil.gd.cn (M.C.); cefbli@soil.gd.cn (F.L.)

<sup>3</sup> School of Geography & Environmental Science, Guizhou Normal University, Guiyang 550001, China; longjian22@gznu.edu.cn

<sup>4</sup> College of Agriculture, Guangxi University, Nanning 530005, China; ljfy1173@126.com (J.L.); gumh@gxu.edu.cn (M.G.)

\* Correspondence: liuchengshuai@vip.gyig.ac.cn; Tel.: +86-851-85891334

† These authors contributed equally to the work.

Received: 18 July 2018; Accepted: 22 August 2018; Published: 24 August 2018



**Abstract:** The interaction between aqueous Fe(II) ( $\text{Fe(II)}_{aq}$ ) and iron minerals is an important reaction of the iron cycle, and it plays a critical role in impacting the environmental behavior of heavy metals in soils. Metal substitution into iron (hydr)oxides has been reported to reduce Fe atom exchange rates between  $\text{Fe(II)}_{aq}$  and metal-substituted iron (hydr)oxides and inhibit the recrystallization of iron (hydr)oxides. However, the environmental behaviors of the substituted metal during these processes remain unclear. In this study, Fe(II)<sub>aq</sub>-induced recrystallization of Cr-substituted goethite (Cr-goethite) was investigated, along with the sequential release behavior of substituted Cr(III). Results from a stable Fe isotopic tracer and Mössbauer characterization studies show that Fe atom exchange occurred between  $\text{Fe(II)}_{aq}$  and structural Fe(III) ( $\text{Fe(III)}_{oxide}$ ) in Cr-goethites, during which the Cr-goethites were recrystallized. The Cr substitution inhibited the rates of Fe atom exchange and Cr-goethite recrystallization. During the recrystallization of Cr-goethites induced by  $\text{Fe(II)}_{aq}$ , Cr(III) was released from Cr-goethite. In addition, Cr-goethites with a higher level of Cr-substituted content released more Cr(III). The highest Fe atom exchange rate and the highest amount of released Cr(III) were observed at a pH of 7.5. Under reaction conditions involving a lower pH of 5.5 or a higher pH of 8.5, there were substantially lower rates of Fe atom exchange and Cr(III) release. This trend of Cr(III) release was similar with changes in Fe atom exchange, suggesting that Cr(III) release is driven by Fe atom exchange. The release and reincorporation of Cr(III) occurred simultaneously during the  $\text{Fe(II)}_{aq}$ -induced recrystallization of Cr-goethites, especially during the late stage of the observed reactions. Our findings emphasize an important role for  $\text{Fe(II)}_{aq}$ -induced recrystallization of iron minerals in changing soil metal characteristics, which is critical for the evaluation of soil metal activities, especially those in Fe-rich soils.

**Keywords:** trace metal release; iron mineral; Fe atom exchange; phase transformation; soil metal activity

## 1. Introduction

Iron (hydr)oxides such as lepidocrocite, goethite, and hematite are common secondary iron minerals in soils. Iron (hydr)oxides rarely occur in a chemically pure form, and usually contain

structural trace metal admixtures in soils, especially in polluted soils with metallic contaminants [1–3]. A number of trace metals, including Al(III), Ti(II), Cr(III), Mn(III), Ni(II), As(III), and Cu(II), were observed to be substituted into the structures of iron (hydr)oxides upon replacing Fe(III) in the lattice [4,5]. In particular, Mn(III) and Al(III) were found to occupy up to 47 mol% and 33 mol%, respectively, of Fe(III) sites within iron (hydr)oxides [3,6]. Similarly, Cr-substituted goethites are also common in natural soil due to the similar ionic radii of Cr(III) (61.5 pm) and Fe(III) (64.5 pm) [4]. Isomorphous substitution of metals in the structures of iron (hydr)oxides can lead to metal immobilization and, therefore, to the formation of stable metal-containing mineral phases, ultimately reducing the activities of iron (hydr)oxides and the bioavailability of metals [3,7,8].

The structural incorporation of trace metals into natural iron (hydr)oxides often results from mineral formation, secondary mineralization reactions, and weathering [9]. Following the formation of these secondary iron minerals, active biogeochemical reaction processes occur, potentially causing the release of trace metals from the mineral structure [10,11], and effectively increasing the mobility and bioavailability of these trace metals. For example, the dissimilatory iron reduction of metal-substituted iron (hydr)oxides by iron-reducing bacteria lead to the release of substituted metals and increases their bioavailability [1,12]. A large scale of trace metals, such as Cu, Cr, Co, Pb, and others, were released accompanied by Fe(II) and dissolved organic matter during the microbial reduction of iron minerals in soils [13]. Additionally, the chemical weathering of secondary iron minerals, such as pyrite, largely increased the mobility of the structurally incorporated trace metals [2]. In general, a wide range of reactions in soil biogeochemical processes, such as microbial redox, element cycle, and physical and chemical weathering, can affect the environmental behaviors and fates of trace metals in soils.

The iron atom exchange between aqueous Fe(II) ( $\text{Fe(II)}_{aq}$ ) and iron (hydr)oxides is the important reaction in the soil iron cycle, as well as dissimilatory Fe(III) reduction and ferrous oxidative mineralization [14–16].  $\text{Fe(II)}_{aq}$ -induced recrystallization of iron (hydr)oxides which occurs during the reaction between  $\text{Fe(II)}_{aq}$  and iron (hydr)oxides was reported to play a critical role in the environmental behaviors of metal contaminants in soils [17–20].  $\text{Fe(II)}_{aq}$ -induced recrystallization of iron (hydr)oxides results in the structural incorporation of coexisting metals through the isomorphous replacement of these metals with the Fe(III) sites of the iron (hydr)oxides [21,22]. Additionally, the crystal rearrangement during the recrystallization leads to the occlusion of metals by the crystal units [17,22]. For example, the unstable iron (hydr)oxide, ferrihydrite, undergoes an efficient phase transformation into more stable phases, including lepidocrocite, goethite, and magnetite, consequently stabilizing various metal ions through structural incorporation [23,24].

Chromium (Cr) is a common metal contaminant in soil. Hexavalent chromium (Cr(VI)) is of increasing concern due to its toxicity and health risks among humans [25,26]. Cr(III) is an essential trace element for man and animals with less mobility and less toxicity, but it becomes a problem when it is released and oxidized to Cr(VI) in soil [27]. Therefore, understanding the environmental behavior of Cr is worthy of consideration, especially that in iron (hydr)oxides in conditions relevant to Fe-rich soils with strong iron cycling. Previous studies found that Cr(III) could be incorporated into goethite [28], changing the thermal and mineral properties of Cr-substituted goethite (Cr-goethite) upon undergoing isomorphous substitution [7], which would further reduce the dissolution of goethites and the release of Cr [11]. Despite the phase of Cr-substituted iron (hydr)oxides being relatively stable following substitution, the release of Cr from Cr-goethites was found during biogeochemical reactions [11]. Approximately 8.46% and 35% of the present Cr were released from 5 mol% Cr-goethites by iron-reducing bacteria and a citrate-bicarbonate solution, respectively [11]. Previous studies also indicated that metals such as Cu(II), Ni(II), Co(II), and Mn(II) could be released from metal-substituted iron (hydr)oxides as a result of the  $\text{Fe(II)}_{aq}$ -induced recrystallization of iron (hydr)oxides [17]. However, the influence of  $\text{Fe(II)}_{aq}$ -induced recrystallization of Cr-goethite on the behavior of Cr is not yet fully understood.

Therefore, in this study, we focused on exploring the influence mechanism of Cr-goethite on the behavior of Cr during the recrystallization induced by  $\text{Fe(II)}_{aq}$ . To achieve this objective, we determined

the Fe atom exchange efficiencies between  $\text{Fe(II)}_{aq}$  and  $\text{Fe(III)}_{oxide}$  in goethites when substituted with various levels of Cr(III). We also identified the crystal phase changes of Cr-goethites and monitored the structural decomposition and release of substituted Cr(III) in goethites during the  $\text{Fe(II)}_{aq}$ -induced recrystallization of Cr-goethites.

## 2. Materials and Methods

### 2.1. Pure Goethite and Cr-Goethite Preparation

Pure goethite and Cr-goethite samples were synthesized with or without Cr(III) substitution using a modification of previously described methods [29]. In brief, 0.5 M  $\text{Cr(NO}_3)_3$  solution was mixed with 150 mL of 5 M KOH in a 1 L polypropylene bottle to obtain an alkaline Cr solution. Then, 50 mL of 1 M  $\text{Fe(NO}_3)_3$  was added to 0, 3.3, 8.4, 30.5, and 75.3 mL of the alkaline Cr solution and brought to 0.3 M KOH with 90, 9, 91.5, 84.5, and 70.5 mL of 5 M KOH in a final volume of 1 L, respectively. Solutions were shaken (by hand) end-over-end daily for 15 s, and aged for 40 days at  $75 \pm 1$  °C.

The amorphous materials of the products were removed through 1 h extraction with 3 M  $\text{H}_2\text{SO}_4$  at 50 °C, centrifuging, and decanting the aqueous phase. Afterward, the products were washed four times with distilled deionized water to remove the electrolytes. Then, the products were dried at 50 °C overnight. Lastly, the samples were gently crushed in an agate mortar, passed through a 200-mesh (150  $\mu\text{m}$ ) sieve, and stored in an anaerobic bag before use. The initial  $[\text{Cr}]:([\text{Cr}] + [\text{Fe}])$  mole ratios of the products were 0, 0.02, 0.05, 0.16, and 0.32, respectively, and the actual molarity percentages were 1.4%, 3.5%, 9.03%, and 10.3%, respectively. The obtained solids are henceforth referred to as pure goethite, 1.4% Cr-goethite, 3.5% Cr-goethite, 9.03% Cr-goethite, and 10.3% Cr-goethite.

For the characterization of  $\text{Fe(II)}_{aq}$ -induced recrystallization of Cr-goethite with Mössbauer spectroscopy, the 9.03% Cr-substituted  $^{56}\text{Fe}$ -goethite samples (9.03% Cr- $^{56}\text{Fe}$  goethite) were prepared from  $^{56}\text{Fe}$  (0) powder (Isoflex, 99.94%) using a modification of previously described methods [3,30]. In brief,  $^{56}\text{Fe}$  (0) was dissolved in 5 M HCl to obtain an Fe(II) stock solution, and the solution was then oxidized using excess 30%  $\text{H}_2\text{O}_2$  to produce Fe(III). Other than using  $^{56}\text{Fe(III)}$  instead of  $\text{Fe(NO}_3)_3$ , all other synthesis parameters were used as described in the above procedure.

### 2.2. Experiments on $\text{Fe(II)}_{aq}$ -Induced Recrystallization of Cr-Goethite

All kinetic experiments were conducted with a Pb catalyst in an anaerobic chamber (Coy LAB, 7%  $\text{H}_2$ /93%  $\text{N}_2$ ), with  $\text{O}_2$  concentrations kept below 1 ppm at 25 °C. All solutions were purged with high-purity  $\text{N}_2$  (~1 L/h) before being transferred to the chamber. This was followed by 24 h of balancing inside the chamber to become equilibrated with the anoxic environment using its anaerobic atmosphere. An  $^{57}\text{Fe}$ -enriched solution of 100 mM  $\text{Fe(II)}_{aq}$  was prepared in 5 M HCl by dissolving enriched  $^{57}\text{Fe}$  (Isoflex,  $^{57}\text{Fe} > 96.0\%$ ) metal in a glass vial.

Batch experiments were conducted to evaluate the  $\text{Fe(II)}_{aq}$ -induced Cr(III) release from Cr-goethites through three microcosm treatments. The first microcosm treatment involved goethites substituted by various levels of Cr(III) (0%, 1.4%, 3.4%, 9.03%, or 10.3%) with 1.0 mM  $^{57}\text{Fe(II)}_{aq}$  at a pH of 7.5, in an effort to study the release of Cr(III) from Cr-goethites induced by  $\text{Fe(II)}_{aq}$ . The second microcosm treatment involved the use of various initial  $^{57}\text{Fe(II)}_{aq}$  concentrations (0.5 mM, 1.0 mM, 1.5 mM, or 2.5 mM) with 9.03% Cr-goethite at a pH of 7.5, in an effort to study the effect of initial  $\text{Fe(II)}_{aq}$  concentrations. The third microcosm treatment involved using 1.0 mM initial  $^{57}\text{Fe(II)}_{aq}$  with 9.03% Cr-goethite at various pH values (5.5, 7.5, and 8.5), in an effort to study the effect of pH. Each reactor contained 2 g/L of solid (pure goethite or Cr-goethite) and 10 mL of 25 mM buffer solution (2-(*n*-morpholino)ethanesulfonic acid (MES) for pH 5.5, 4-(2-hydroxyethyl)-1-piperazineethanesulfonic acid (HEPES) for pH 7.5, and tris(hydroxymethyl)aminomethane (TRIS) for pH 8.5) with 25 mM KBr as a background electrolyte. All reactors were wrapped in Al foil and placed on an end-over-end rotator (installed inside the anaerobic chamber) to keep the suspension mixed.

Three reactors were sacrificed for isotopic and chemical analyses at specified time points (0, 0.125, 1, 4, 8, 18, and 30 days) for sampling.

Firstly, a 5 mL suspension from each reactor was placed into a 15 mL centrifuge tube and centrifuged at  $10,000 \times g$  for 10 min, before being immediately returned to the chamber. The supernatant was decanted into a syringe and filtered using 0.22  $\mu\text{m}$  filters. The filtrate was acidified to 2% HCl and saved for analysis of the concentrations of  $\text{Cr(III)}_{aq}$ ,  $\text{Fe(II)}_{aq}$ , and total  $\text{Fe}_{aq}$ , and the isotopic composition of Fe. The goethite solids were resuspended in 5 mL of 0.4 M HCl for 10 min to remove the sorbed  $\text{Cr(III)}$ ,  $\text{Fe(II)}$ , and  $\text{Fe(III)}$ . Afterward, the centrifugation and filtration steps were repeated to isolate the aqueous phase. The  $\text{Fe(II)}$  and  $\text{Cr(III)}$  in this 0.4 M HCl extract are henceforth referred to as  $\text{Fe(II)}_{\text{extr}}$  and  $\text{Cr(III)}_{\text{extr}}$ , respectively. Remaining goethite solids were completely dissolved in 4 M HCl. The  $\text{Fe(II)}$  and  $\text{Cr}$  in this 4 M HCl extract are henceforth referred to as  $\text{Fe(II)}_{\text{solid}}$  and  $\text{Cr(III)}_{\text{solid}}$ , respectively. Subsamples of the aqueous solution and the sequential extractions were analyzed for  $\text{Fe(II)}$  and  $\text{Fe(III)}$ . Goethite solids were collected from the remaining 5 mL of the original reactor suspension for phase analysis.

### 2.3. Analyses of $\text{Fe(II)}$ , $\text{Fe(III)}$ , and $\text{Cr(III)}$ Concentrations, and Fe Isotope Composition

$\text{Fe(II)}$  concentrations were determined using the 1,10-phenanthroline (1 g/L) method, with masking of  $\text{Fe(III)}$  by fluoride when required [31].  $\text{Fe(III)}$  concentrations were determined through reduction of  $\text{Fe(III)}$  with hydroxylamine hydrochloride to  $\text{Fe(II)}$ , and the  $\text{Fe(III)}$  concentration was calculated using the difference. The Cr contents in Cr-goethites were determined through solid digestion of 20 mg of Cr-goethites in a mixture of 10 mL of 20%  $\text{HNO}_3$  and 5% HCl (trace metal grade, Fisher Scientific, Pittsburgh, PA, USA). Cr concentrations were measured via inductively coupled plasma optical emission spectrometry (ICP-OES, Perkin-Elmer Optima 8000, Perkin Elmer, Waltham, MA, USA) with one standard sample per 10 samples.

Iron isotope analyses were carried out using inductively coupled plasma mass spectrometry (ICP-MS, PerkinElmer NexION 300D, Perkin Elmer, Waltham, MA, USA), operating in collision cell mode with a glass concentric nebulizer and a high-efficiency particulate air (HEPA)-filtered auto sampler. The polyatomic argide molecules ( $\text{ArO}^+$  and  $\text{ArN}^+$ ) were eliminated with a collision cell gas containing 93% He and 7%  $\text{H}_2$  (>99.999% pure) with a flow rate of 1 mL/min. All solutions were diluted to 1  $\mu\text{m}$  Fe in 2%  $\text{HNO}_3$  (trace metal grade). Fe isotope fractions ( $f$ ) were calculated by dividing the counts in each isotope channel by the sum of the total counts across all four channels (masses of 54, 56, 57, and 58) [32]. Fe atom exchange rates were calculated with the following equation [33,34]:

$$\text{Fe atom exchange (\%)} = \frac{N_{aq} \times (f_{aq}^i - f_{\text{Fe(II)}}^t)}{N_{\text{Goe}}^{\text{Tot}} \times (f_{\text{Fe(II)}}^t - f_{\text{Goe}}^i)} \times 100 \quad (1)$$

where  $N_{aq}$  and  $N_{\text{Goe}}^{\text{Tot}}$  are the moles of  $\text{Fe(II)}_{aq}$  in the system and total moles of Fe in the goethite (either pure goethite or Cr-goethite), respectively.  $f_{aq}^i$  and  $f_{\text{Goe}}^i$  are the initial isotopic fractions of  $\text{Fe(II)}_{aq}$  and goethite (either pure goethite or Cr-substituted goethite), respectively.  $f_{\text{Fe(II)}}^t$  is the isotopic fraction of aqueous  $\text{Fe(II)}$  at time  $t$ .

### 2.4. Mineral Characterization

Cr K-edge extended X-ray absorption fine structure (EXAFS) spectroscopy was collected in fluorescence for 10.3% Cr-goethite solids at the BL16A1 beamline at the National Synchrotron Radiation Research Center (NSRRC) Taiwan light source (TLS). The electron storage ring operated at 1.504 GeV with currents ranging from 300 mA immediately after filling to a refill current of 110 mA. The morphologies and crystallite sizes of pure goethite and 9.03% Cr-goethites before and after reaction with  $\text{Fe(II)}_{aq}$  for 30 days were analyzed using a JEOL JSM-7001F field emission scanning electron microscope (SEM, JEOL Ltd., Tokyo, Japan), operating at 30 keV. The crystal structures of pure

goethite and Cr-goethite were analyzed via X-ray diffraction (XRD) using a D8 advance diffractometer (Bruker AXS, Bruker Corporation, Billerica, MA, USA) with a Lynxeye detector, operating at 40 kV and 40 mA with Cu-K $\alpha$  radiation at room temperature. Mössbauer spectroscopy of 9.03% Cr-goethite solids before and after reaction with  $^{57}\text{Fe}(\text{II})_{\text{aq}}$  for 30 days were collected at low temperature (13 K) using a  $^{57}\text{Co}/\text{Rh}$   $\gamma$ -radiation source with a constant acceleration mode (Wissel MS-500, WissEl, Kleve, Germany). The isomer shifts were given relative to those of  $\alpha$ -Fe at room temperature. Solid samples were collected on a 0.22  $\mu\text{m}$  filter before being sealed between two pieces of adhesive Kapton tape to avoid air oxidation. The spectra were fitted using the Recoil 1.04 software (Ottawa, ON, Canada) with Lorentzian Site Analysis.

### 3. Results and Discussion

#### 3.1. Properties of Cr-Goethite

The XRD patterns of the prepared pure goethite and Cr-goethites with various Cr(III) substitution contents were determined (Figure 1). The XRD patterns of all samples showed characteristic (110) and (120) peaks at  $2\theta$  of  $\sim 21^\circ$  and  $\sim 26^\circ$ , which were consistent with the standard pattern of goethite. The results suggest that the incorporated Cr(III) amount did not change the structure of goethite and did not lead to the formation of a new mineral. When compared with the pattern of pure goethite, a displacement of the total broadband toward smaller  $2\theta$  values was observed in the pattern of Cr-goethites with increasing Cr(III) content, and the unit cell parameters (a, b, c) of Cr-goethite decreased from 4.614 to 4.608  $\text{\AA}$ , 9.965 to 9.942  $\text{\AA}$ , and 3.024 to 3.019  $\text{\AA}$ , respectively (Table 1). These results revealed that Cr(III) was incorporated in the goethite structure, which resulted in the change of unit cell parameters [35,36]. The SEM results were consistent with the XRD analyses, showing that the crystalline morphology of 9.03% Cr-goethite was generally needlelike, but more broken than that of pure goethite (Figure 2). The EXAFS characterization results also confirmed the structural substitution of Cr(III) in the goethite. As shown in Figure 3a, the prepared 10.3% Cr-goethite achieved a Cr-O distance of 1.98  $\text{\AA}$ , which was consistent with the Cr-O distance value reported in the previous study [28]. The X-ray absorption near edge structure (XANES) spectra of 10.3% Cr-goethite was similar to that of Cr(III), suggesting no Cr oxidation states such as Cr(VI) in this study (Figure 3b).

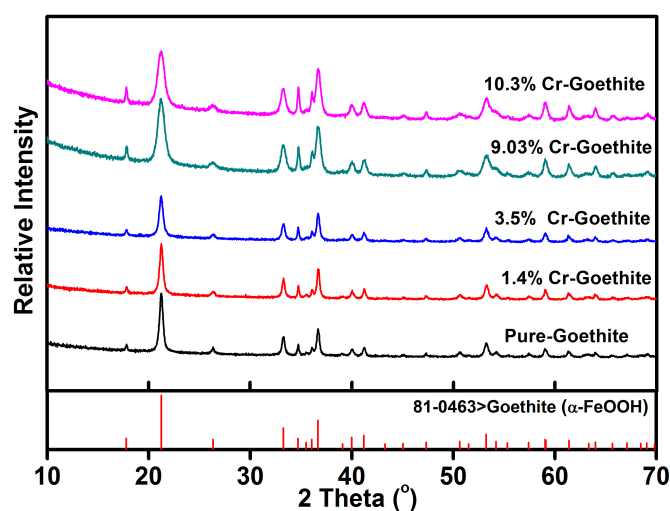


**Figure 1.** X-ray diffraction (XRD) patterns of the prepared pure goethite and Cr-substituted goethite (Cr-goethite) samples.

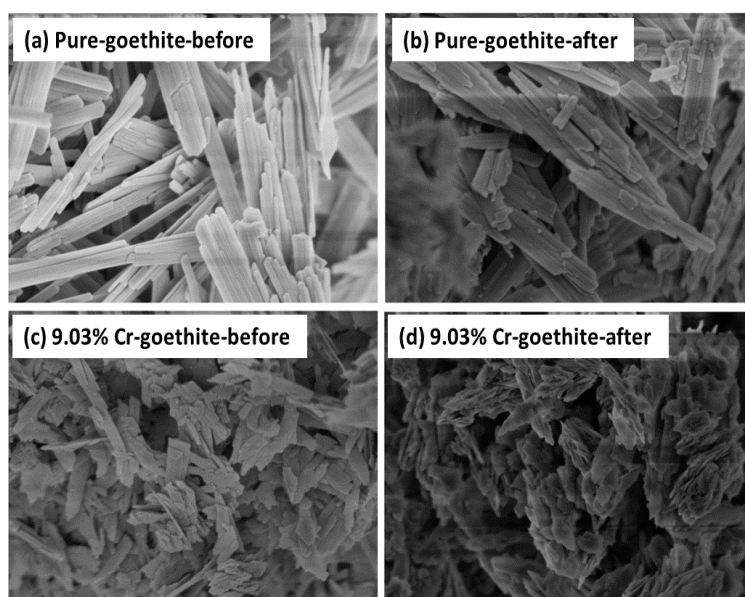


**Figure 2.** Scanning electron microscopy (SEM) images of pure goethite and 0.09 ratio of [Cr]:([Cr] + [Fe]) Cr-goethite (9.03% Cr-goethite) before and after reaction with  $Fe(II)_{aq}$ . (a) Pure goethite, (b) pure goethite after reaction for 30 days, (c) 9.03% Cr-goethite, and (d) 9.03% Cr-goethite after reaction for 30 days. Conditions:  $[Fe(II)_{aq}] = 1 \text{ mM}$ ,  $[goethite] = 2 \text{ g/L}$ , pH 7.5 controlled with 25 mM 4-(2-hydroxyethyl)-1-piperazineethanesulfonic acids (HEPES)/KBr.

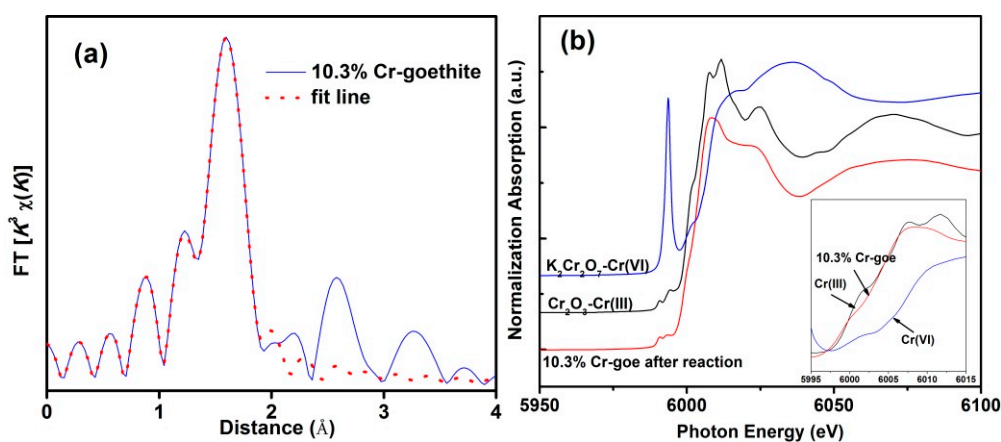


**Figure 3.** (a)  $k^3$ -weighted extended X-ray absorption fine structure (EXAFS) spectra (solid line) and linear combination fits (dotted line) for 10.3% Cr-substituted goethite, (b) the X-ray absorption near edge structure (XANES) spectra for the Cr k-edge of 10.3% Cr-goethite.

**Table 1.** The lattice parameters of pure goethite and Cr-substituted goethites (Cr-goethites) calculated from their X-ray diffraction (XRD) patterns presented in Figure 1. Cr-substituted goethites are represented by numbers defining their ratios of  $[Cr]:([Cr] + [Fe])$ .

Lattice Parameters	Pure Goethite	1.4% Cr-Goethite	3.5% Cr-Goethite	9.03% Cr-Goethite	10.3% Cr-Goethite
a	4.614	4.613	4.612	4.609	4.608
b	9.965	9.958	9.957	9.948	9.942
c	3.024	3.021	3.023	3.020	3.019

To further quantify the accuracy of substituted Cr(III) contents in the prepared samples, chemical analyses of  $\text{Cr(III)}_{aq}$ ,  $\text{Cr(III)}_{extr}$ , and  $\text{Cr(III)}_{solid}$  concentrations were conducted in the Cr-goethites. The results showed that neither  $\text{Cr(III)}_{aq}$  nor  $\text{Cr(III)}_{extr}$  was detected, indicating that all of the Cr(III) was structurally incorporated into the goethites. The actual percentages of Cr(III) in the various Cr-goethites were all lower than the calculated ratios of Cr(III) before synthesis. This was because not all the added Cr(III) was incorporated into the goethites due to the pH value, temperature, aging time, and other factors during the preparation [3].

### 3.2. Influence of Cr-Substitution on Fe Atom Exchange and Electron Transfer between $\text{Fe(II)}_{aq}$ and Goethites

To explore the influence of Cr-substitution on Fe atom exchange and electron transfer between  $\text{Fe(II)}_{aq}$  and goethite, all Cr-goethites with naturally abundant stable Fe isotopes were combined with 1 mM of  $^{57}\text{Fe(II)}_{aq}$  at a pH of 7.5. Fractional changes in the levels of the four stable Fe isotopes of  $\text{Fe(II)}_{aq}$  during the reaction of  $\text{Fe(II)}_{aq}$  with the Cr-goethites are shown in Figure 4. In all five treatments with Cr-goethites with various contents of substituted Cr(III), the compositions of  $^{57}\text{Fe(II)}$  ( $f^{57}\text{Fe}$ ) in  $\text{Fe(II)}_{aq}$  decreased substantially during the first day, and continued decreasing slowly on subsequent days. Simultaneously, the compositions of  $^{56}\text{Fe(II)}$  ( $f^{56}\text{Fe}$ ) in all five treatments increased quickly during the first day, and then continued increasing slowly on subsequent days. These results suggest that Fe atom exchange occurred between  $\text{Fe(II)}_{aq}$  and  $\text{Fe(III)}_{oxide}$  of the goethites, in which some  $^{57}\text{Fe}$  atoms of  $\text{Fe(II)}_{aq}$  entered into the structure of pure goethite and Cr-goethite, while some Fe atoms from the natural isotopic Fe (i.e.,  $^{56}\text{Fe(II)}$  from iron oxides) of the pure goethite and Cr-goethites were released into the solution as  $\text{Fe(II)}_{aq}$  [33,34]. For the pure goethite and Cr-goethite, the composition changes in  $^{57}\text{Fe(II)}$  and  $^{56}\text{Fe(II)}$  were substantially different. The increase of  $f^{56}\text{Fe}$  in  $\text{Fe(II)}_{aq}$  in pure goethite was much higher than that for the Cr-goethite. To further quantify the Fe atom exchange, the change rates in all treatments were calculated using the Equation (1) [32,33] (Figure 5). The Fe atom exchange rate in the pure goethite reached 19.17% following reaction with  $\text{Fe(II)}_{aq}$  for 30 days, which was much higher than that for all other Cr-goethites. For the Cr-goethite with various contents of substituted Cr(III), the Fe atom exchange rates were also different. The lower rates were obtained in Cr-goethites with higher Cr contents. These results suggest that the Cr-substitution in goethites inhibited the Fe atom exchange rate between  $\text{Fe(II)}_{aq}$  and  $\text{Fe(III)}_{oxide}$ .

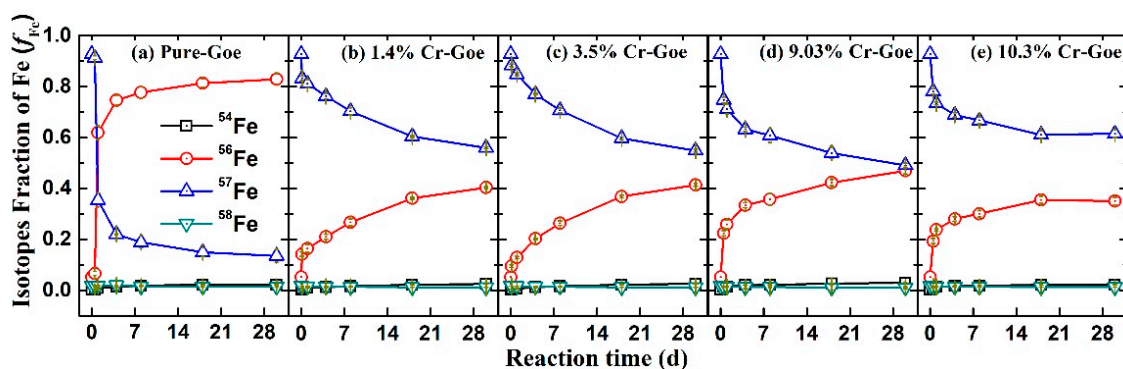


**Figure 4.** Changes in the four Fe isotopic compositions in aqueous solution during the  $\text{Fe(II)}_{aq}$ -induced recrystallization of (a) pure goethite, (b) 1.4% Cr-goethite, (c) 3.5% Cr-goethite, (d) 9.03% Cr-goethite, and (e) 10.3% Cr-goethite. Conditions:  $[\text{Fe(II)}_{aq}] = 1 \text{ mM}$ ,  $[\text{goethite}] = 2 \text{ g/L}$ , pH 7.5 controlled with 25 mM HEPES/KBr.

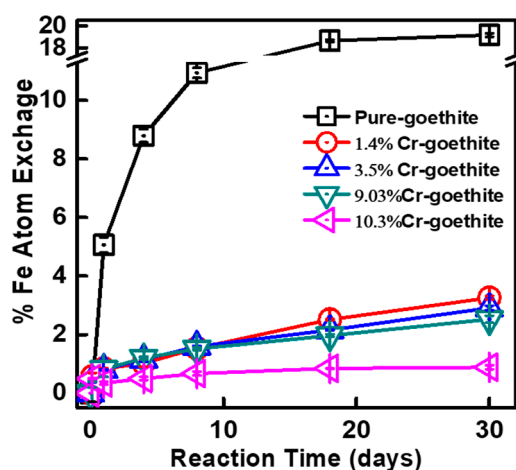


**Figure 5.** Changes in Fe atom exchange rates during the  $\text{Fe(II)}_{aq}$ -induced recrystallization of pure goethite, 1.4% Cr-goethite, 3.5% Cr-goethite, 9.03% Cr-goethite, and 10.3% Cr-goethite over 30 days. Conditions:  $[\text{Fe(II)}_{aq}] = 1 \text{ mM}$ ,  $[\text{goethite}] = 2 \text{ g/L}$ , pH 7.5 controlled with 25 mM HEPES/KBr.

The rate of Fe atom exchange between the  $\text{Fe(II)}_{aq}$  and  $\text{Fe(III)}_{oxide}$  of iron (hydr)oxides were reported to be affected by various structural properties, for example, structural defects, particle sizes, and solid electron conductivity [6,30,32,37,38]. Notini et al. [28] reported that surface defects of the goethite played an important role in Fe(II)-goethite redox interactions, and that the oxidation of  $\text{Fe(II)}_{aq}$  by goethite was kinetically inhibited on structurally perfect surfaces. Latta et al. [37] found that Al-substitution in goethites reduced the Fe atom exchange rate between  $\text{Fe(II)}_{aq}$  and Al-goethites, and that the reduced electron conductivity in the bulk mineral resulted from the surface Al-coating. As shown in Figure 2, the morphology of Cr-goethites transformed from an acicular nature into a rod-like nature with a smaller diameter than that of pure goethite, which would result in a reduction in conductivity [39]. Based on previous reports and our results, the lower Fe atom exchange rates in goethite with Cr-substitutions were expected to have a higher degree of crystallinity and lower bulk conductivity. The higher contents of substituted Cr led to more severe inhibition of the Fe atom exchange.

To further confirm the extent of Fe atom exchange and the recrystallization of Cr-goethites induced by  $\text{Fe(II)}_{aq}$ , the  $^{57}\text{Fe}$  isotope specificity of Mössbauer spectroscopy was used to track Fe atom transfer. Mössbauer-invisible  $^{56}\text{Fe}$  was used to prepare 9.03% Cr-goethite ( $\text{Cr-}^{56}\text{goethite}$ ), before reacting it with 1 mM  $^{57}\text{Fe(II)}_{aq}$ . The solid samples were collected before and after the reaction for analysis using Mössbauer spectroscopy. The results showed that the characteristic sextets were obviously absent from the Mössbauer spectra for  $\text{Cr-}^{56}\text{goethite}$  before the reaction (Figure 6a) [16]. Following 30 days of reaction with  $^{57}\text{Fe(II)}_{aq}$ , the Mössbauer spectra of the reacted solid was recorded, and they revealed two prominent Fe(III) sextets (chemical shift (CS)  $\approx 0.482 \text{ mm/s}$ , quadrupole splitting (QS)  $\approx -0.112 \text{ mm/s}$ , and CS  $\approx 0.459 \text{ mm/s}$ , QS  $\approx -0.142 \text{ mm/s}$ ) consistent with goethite (Figure 6b), suggesting that some of the  $^{57}\text{Fe(II)}_{aq}$  was oxidized and entered into the structure of goethite resulting in the formation of  $^{57}\text{goethite}$ . The results clearly suggest the occurrence of electron transfer and Fe atom exchange between  $\text{Fe(II)}_{aq}$  and Cr-goethite [30]. From the Mössbauer characterization results, we can also find that new goethite consisting of  $^{57}\text{Fe}$  was formed in the  $\text{Cr-}^{56}\text{goethite}$  following reaction with  $^{57}\text{Fe(II)}_{aq}$ . The Cr-goethite was recrystallized through induction by  $\text{Fe(II)}_{aq}$ , while the recrystallized products had a crystalline phase similar to that of the initial mineral.

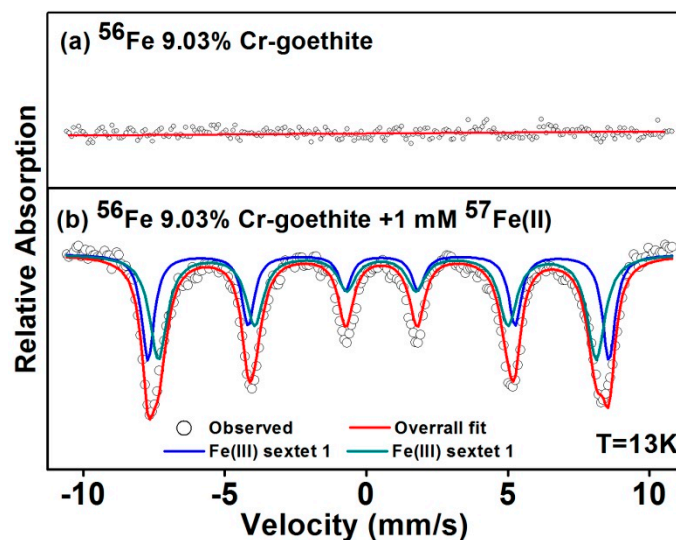


**Figure 6.** Mössbauer spectra of (a) unreacted 9.03% Cr-<sup>56</sup>Fe goethite, and (b) 9.03% Cr-<sup>56</sup>Fe goethite following reaction with 1.0 mM <sup>57</sup>Fe(II)<sub>aq</sub> for 30 days.

### 3.3. Cr(III) Release during the Fe(II)<sub>aq</sub>-Induced Recrystallization of Cr-Goethites

The concentrations of Cr(III)<sub>aq</sub>, Cr(III)<sub>extr</sub>, and Cr(III)<sub>solid</sub> were determined to investigate the release behavior of Cr(III) during Fe(II)<sub>aq</sub>-induced recrystallization of Cr-goethites (Figure 7). It should be pointed out that the  $K_{sp}$  value of Cr(OH)<sub>3</sub> is  $6.3 \times 10^{-31}$  [40], and the potentially released Cr cannot exist as aqueous form at the reaction pH of 7.5. Therefore, no Cr(III)<sub>aq</sub> was observed across all analyses in our study. As shown in Figure 7a, the concentration of Cr(III)<sub>extr</sub> quickly increased from 0 to 0.515 mg/g, 2.89 mg/g, 20.65 mg/g, and 29.08 mg/g in the first 3 h of treatments with 1.4% Cr-goethite, 3.5% Cr-goethite, 9.03% Cr-goethite, and 10.3% Cr-goethite, respectively. After reaction for 4 days, the concentrations of Cr(III)<sub>extr</sub> in all treatments decreased slowly. However, the changes in the concentration of Cr(III)<sub>solid</sub> showed a contrary trend for each treatment (Figure 7b). In all five treatments, the concentrations of Cr(III)<sub>solid</sub> decreased quickly in the first three hours, and kept decreasing until the fourth day. After the fourth day, the concentrations then slowly increased. These results demonstrate that, during the Fe(II)<sub>aq</sub>-induced recrystallization of Cr-goethites, the structural Cr(III) in the goethites was released and existed as the adsorbed form. We also found that the trends of the changes in concentration of Cr(III) release were similar to those of the changes in concentration of aqueous <sup>56</sup>Fe (i.e., increased quickly before slowly increasing to a plateau). More Cr(III) was released in treatments with higher-substituted Cr-goethites. The highest released amount of Cr(III)<sub>extr</sub> in the treatment of 10.3% Cr-goethite also obtained the lowest Fe atom exchange rate (Figure 5). A previous study found that the iron dissolution from goethite during the electron transfer and iron atom exchange between Fe(II)<sub>aq</sub> and Fe(III)<sub>oxide</sub> was due to Fe-O bonds broken [41]. These results suggest that the release of Cr(III) was a result of the rupture of Cr(III)-related bonds due to electron transfer between Fe(II)<sub>aq</sub> and Fe(III)<sub>oxide</sub>, and the consequent recrystallization of Cr-goethites [10,18]. Additionally, the surface sites of iron (hydr)oxide occupied by heavy metals led to the inhibition of further recrystallization of iron (hydr)oxide [12,35]. Therefore, the results of the present study suggest that the recrystallization of Cr-goethites resulted in the rupture of Cr-related bonds and the release of Cr(III). Due to the low  $K_{sp}$  value of Cr(III), the released Cr(III) cannot exist in aqueous form, but can exist as the adsorbed form on the surface of goethites, further inhibiting the reaction between Fe(II)<sub>aq</sub> and Fe(III)<sub>oxide</sub>, and reducing the rate of Fe atom exchange. The trends of Cr<sub>extr</sub> over time under various initial Fe(II)<sub>aq</sub> concentrations were similar. The concentrations of Cr<sub>extr</sub> initially increased before decreasing over time. The increase in Cr<sub>extr</sub> concentration at the beginning of the reactions indicates structural Cr being released from the Cr-substituted goethite. Along with further

Fe(II)<sub>aq</sub>-induced recrystallization of goethites, some of the adsorbed Cr(III) was then reincorporated into the recrystallized goethite [23]. As shown in Figure 7, the concentration of Cr<sub>extr</sub> decreased, while the concentration of Cr<sub>solid</sub> increased after four days of reaction.

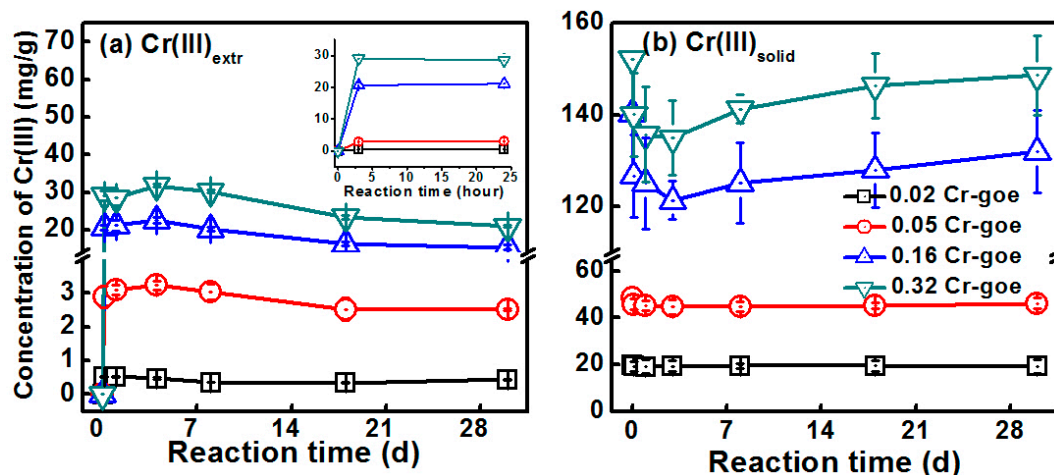


**Figure 7.** The concentrations of (a) Cr(III)<sub>extr</sub> and (b) Cr(III)<sub>solid</sub> during the Fe(II)<sub>aq</sub>-induced recrystallization of 1.4% Cr-goethite, 3.5% Cr-goethite, 9.03% Cr-goethite, and 10.3% Cr-goethite over 30 days. Conditions: [Fe(II)<sub>aq</sub>] = 1 mM, [goethite] = 2 g/L, pH 7.5 controlled with 25 mM HEPES/KBr.

#### 3.4. Effects of pH and Initial Fe(II)<sub>aq</sub> Concentration on Cr(III) Release during the Fe(II)<sub>aq</sub>-Induced Recrystallization of Cr-Goethites

Environment factors (e.g., pH [33], initial Fe(II)<sub>aq</sub> concentration [23], and particle size [32]) have substantial effects on the interplay between the Fe(II)<sub>aq</sub> and Fe(III)<sub>oxide</sub> of iron (hydr)oxide, which further affects the release behavior of Cr(III) in Cr-goethites. To obtain deep insight into the effect of Fe(II)<sub>aq</sub>-induced recrystallization of goethites on the release behavior of Cr(III), we investigated the effects of pH and initial Fe(II)<sub>aq</sub> concentration on Cr(III) release during the Fe(II)<sub>aq</sub>-induced recrystallization of Cr-goethites.

To study the effect of pH on the Fe(II)<sub>aq</sub>-induced recrystallization of Cr-goethites, buffered pH conditions of 5.5, 7.5, and 8.5 were used in experiments with 9.03% Cr-goethite. Figure 8a shows the Fe atom exchange rates under various pH conditions. The rates of Fe atom exchange were 1.02%, 2.52%, and 1.16% in 30-day reactions with pH values of 5.5, 7.5, and 8.5, respectively. This result suggests that, beyond the low Fe atom exchange rates in the 9.03% Cr-goethites, changes in pH conditions had a substantial effect on the Fe atom exchange between Fe(II)<sub>aq</sub> and Fe(III)<sub>oxide</sub>. At a pH of 7.5, Cr-goethites achieved the largest amount of Fe atom exchange among the three pH value conditions. At a pH of 5.5, a smaller proportion of Fe(II)<sub>aq</sub> was sorbed onto the surface of goethites due to the high point of zero charge (7.0 to 8.5) of goethite [42], which reduced the energetics of electron transfer between Fe(II)<sub>aq</sub> and Fe(III)<sub>oxide</sub> in Cr-goethites [33,43,44]. Therefore, substantially less Fe atom exchange occurred over 30 days at a pH of 5.5 when compared with that at a pH of 7.5. When the sample was at a pH of 8.5, the amount of Fe(II)<sub>aq</sub> sorbed onto the surface of goethites exceeded the theoretical surface site capacity and formed multilayer coverage, ultimately leading to surface passivation and the further inhibition of electron transfer between Fe(II)<sub>aq</sub> and Fe(III)<sub>oxide</sub> [32]. These results suggest that Fe(II) sorbed onto the surface of goethites plays an important role in Fe atom exchange between the Fe(II)<sub>aq</sub> and Fe(III)<sub>oxide</sub> of Cr-goethites.

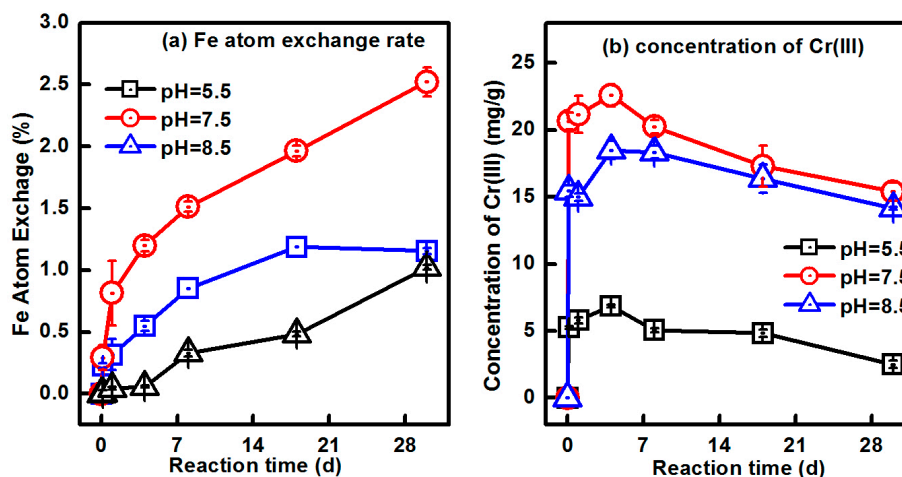


**Figure 8.** Changes in (a) Fe atom exchange percentage and (b) Cr(III)<sub>extr</sub> concentrations during the Fe(II)<sub>aq</sub>-induced recrystallization of 9.03% Cr-goethite over 30 days under various pH (5.5, 7.5, and 8.5) conditions.

The variation in Fe atom exchange rates between the Fe(II)<sub>aq</sub> and Fe(III)<sub>oxide</sub> of Cr-goethites under various pH conditions also led to different Cr(III) release behaviors. As shown in Figure 8b, the trends in Cr(III)<sub>extra</sub> concentration were similar for all three treatments (i.e., increasing quickly until a peak value before decreasing slowly). The highest concentration of Cr(III)<sub>extra</sub> was found at a pH of 7.5, while the lowest level of Cr(III) release was observed at a pH of 5.5. The order of Cr(III) release levels from Cr-goethites was consistent with that of the Fe atom exchange in treatments at a pH of 5.5, 7.5, and 8.5 (Figure 8). More Cr(III) was released from Cr-goethite at a treatment with a higher Fe atom exchange rate. Iron (hydr)oxide is dynamic during the interplay between Fe(II)<sub>aq</sub> and Fe(III)<sub>oxide</sub>, and the quick exchange between Fe(II)<sub>aq</sub> and Fe(III)<sub>oxide</sub> in Cr-goethites leads to increased recrystallization of Cr-goethites [32]. This process consequently enhances the possibilities of Cr-related bond rupture during the crystallization of Cr-goethites, further leading to more Cr(III) released from Cr-goethites. Therefore, more Cr(III) was released from Cr-goethite at pH 7.5 condition, which had a higher Fe atom exchange rate than that of pH 5.5 and 8.5.

To explore the effect of various initial concentrations of Fe(II)<sub>aq</sub> on the Fe atom exchange and Cr(III) release during the Fe(II)<sub>aq</sub>-induced recrystallization of Cr-goethites, 9.03% Cr-goethite was exposed to Fe(II)<sub>aq</sub> with a series of concentrations (0.5 mM, 1 mM, 1.5 mM, and 2.5 mM). The Fe atom exchange rates were 0.43%, 2.52%, 1.92%, and 1.16% in treatments with 0.5 mM, 1.0 mM, 1.5 mM, and 2.5 mM initial Fe(II)<sub>aq</sub>, respectively (Figure 9a). When the initial concentrations of Fe(II)<sub>aq</sub> were greater than 1.0 mM, the Fe atom exchange rates decreased with increasing Fe(II)<sub>aq</sub>. When Fe(II)<sub>aq</sub> coexists with iron (hydr)oxide, Fe(II)<sub>aq</sub> is sorbed onto the surface of iron (hydr)oxide, and a potential gradient is formed. Then, electrons are transferred from the Fe(II)<sub>aq</sub> to the bulk iron (hydr)oxide mineral [16]. During this process, oxidative Fe(II)<sub>aq</sub> uptake occurs on the surface of iron (hydr)oxide. The transferred electrons migrate within the goethite structure, leading to the dissociation of iron (hydr)oxides [16,45–47]. Sorbed Fe(II) is one of the most important driving forces for the interplay between Fe(II)<sub>aq</sub> and Fe(III)<sub>oxide</sub> [32,33,46]. When the amount of sorbed Fe(II) is below the capacity of the monolayer coverage of goethite, Fe(II) sorption is proportional to the amount of Fe(II)<sub>aq</sub> added [32]. Additional Fe(II)<sub>aq</sub> would lead to an increase in sorbed Fe(II), and modify the electrostatic surface potential of goethite responsible for bulk conduction. Consequently, electron transfer between Fe(II)<sub>aq</sub> and Fe(III)<sub>oxide</sub> accelerates, resulting in increased rates of Fe atom exchange [32,45,47]. However, increases in sorbed Fe(II) beyond the capacity of the monolayer coverage can result in Fe(II) surface passivation, which prevents electron inject from outer-sphere to inner-sphere geometry and neutralizes the potential gradient on the surface of the goethite, and further inhibits the exchange between Fe(II)<sub>aq</sub>

and  $\text{Fe(III)}_{\text{oxide}}$  [46–50]. Based on the above results concerning Cr(III) release, the release of Cr(III) from Cr-goethite is considered to be dependent on Fe atom exchange and the efficiency of  $\text{Fe(II)}_{\text{aq}}$ -induced recrystallization of Cr-goethite [49]. As such, the highest level of Cr(III) release was observed in the treatment with 1.0 mM initial  $\text{Fe(II)}_{\text{aq}}$  (Figure 9b), in which the highest percentage of Fe atom exchange between  $\text{Fe(II)}_{\text{aq}}$  and  $\text{Fe(III)}_{\text{oxide}}$  in Cr-goethite was also observed (Figure 9a).

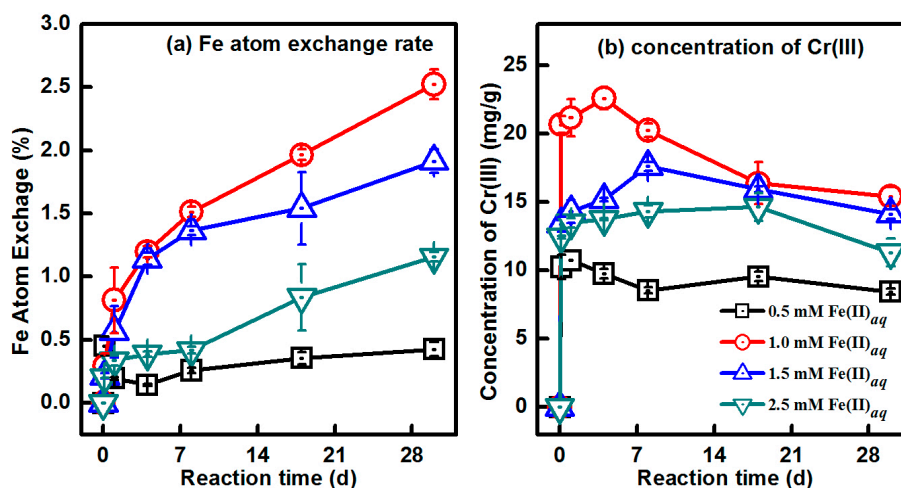


**Figure 9.** Changes in (a) Fe atom exchange percentage and (b)  $\text{Cr(III)}_{\text{extr}}$  concentrations during the  $\text{Fe(II)}_{\text{aq}}$ -induced recrystallization of 9.03% Cr-goethite over 30 days with 0.5 mM, 1.0 mM, 1.5 mM, and 2.0 mM of initial  $\text{Fe(II)}_{\text{aq}}$ .

### 3.5. Cr Release Mechanisms during $\text{Fe(II)}_{\text{aq}}$ -Induced Recrystallization of Cr-Goethite

The coexisting  $\text{Fe(II)}_{\text{aq}}$  with Cr-goethite resulted in electron transfer and Fe atom exchange between  $\text{Fe(II)}_{\text{aq}}$  and  $\text{Fe(III)}_{\text{oxide}}$ , which further induced the recrystallization of Cr-goethites (Figures 4 and 6). During the recrystallization of Cr-goethite induced by  $\text{Fe(II)}_{\text{aq}}$ , Cr(III) was released from the Cr-goethite and partly reincorporated into the goethite (Figure 7). Fe atom exchange between  $\text{Fe(II)}_{\text{aq}}$  and  $\text{Fe(III)}_{\text{oxide}}$  is the driving force for the recrystallization of iron (hydr)oxide, which further results in the release of metals from metal-substituted iron (hydr)oxide [18]. Metals were released during the recrystallization of metal-substituted iron (hydr)oxide by the displacement of surface associated metals by  $\text{Fe(II)}_{\text{aq}}$  [10]. The reductive dissolution during electron transfer and atom exchange between  $\text{Fe(II)}_{\text{aq}}$  and metal-substituted iron (hydr)oxide also could cause the metals' release from metal-substituted iron oxide [17]. Figure 7 shows that the highest amount of Cr release occurred in the 10.3% Cr-goethite treatment with the lowest Fe atom exchange rate, demonstrating that the release of Cr(III) in this study was substantially caused by Cr-related bond rupture and the dissociation of Cr(III) from Cr-goethites. Varying degrees of Cr(III) release were found during the interplay between  $\text{Fe(II)}_{\text{aq}}$  and  $\text{Fe(III)}_{\text{oxide}}$  under various conditions (e.g., changes in pH value and the initial concentration of  $\text{Fe(II)}_{\text{aq}}$ ). More Cr(III) was released from Cr-goethites in treatments with higher Fe atom exchange rates (Figures 8 and 9).

Based on the above results and discussions, the structural behavior of Cr during  $\text{Fe(II)}_{\text{aq}}$ -induced recrystallization of Cr-goethites has three possible mechanistic stages (Figure 10). Firstly,  $\text{Fe(II)}_{\text{aq}}$  is sorbed onto the surface of Cr-goethite, forming a potential gradient. Secondly, electron transfer occurs between  $\text{Fe(II)}_{\text{aq}}$  and  $\text{Fe(III)}_{\text{oxide}}$  in goethite, along with Fe atom exchange, leading to the crystallization of Cr-goethites, ultimately resulting in Cr(III) release caused by Cr-related bond rupture and the dissociation of Cr-goethites during recrystallization. Thirdly, the reincorporation of Cr(III) into goethites occurs during the  $\text{Fe(II)}_{\text{aq}}$ -induced recrystallization process.

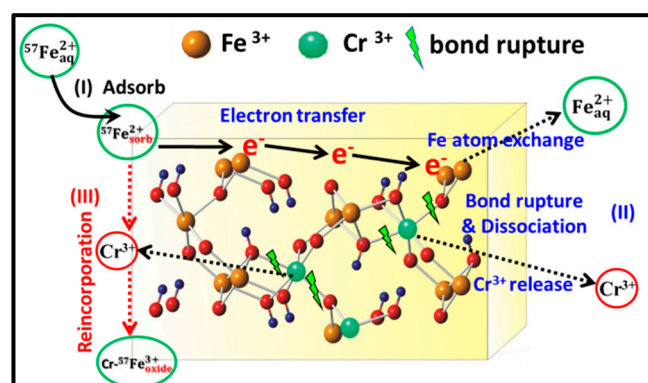


**Figure 10.** Schematic diagram of the behavior of Cr during the recrystallization of Cr-goethite induced by  $\text{Fe(II)}_{aq}$ .

#### 4. Conclusions

In this study, the release of Cr(III) from Cr-goethites was investigated during the recrystallization process induced by  $\text{Fe(II)}_{aq}$  under various conditions. The results show that Cr substitution inhibited Fe atom exchange during  $\text{Fe(II)}_{aq}$ -induced recrystallization of Cr-goethites. The Fe atom exchange between the  $\text{Fe(II)}_{aq}$  and  $\text{Fe(III)}_{oxide}$  in the Cr-goethites resulted in a release of Cr(III). Additionally, Cr(III) was reincorporated into the goethites during the recrystallization process at a later reaction stage. The trends of Fe atom exchange rates under various pH conditions and initial concentrations of  $\text{Fe(II)}_{aq}$  were similar to those observed for the changes in Cr(III) release behavior. More Cr(III) was released from Cr-goethite in the treatment involving higher Fe atom exchange rates, suggesting that the Fe atom exchange played an important role in the release of Cr(III). Cr(III) release was caused primarily by Cr-related bond rupture and the dissociation of Cr-goethites. The pH conditions and initial  $\text{Fe(II)}_{aq}$  concentrations also affected Cr(III) release in the  $\text{Fe(II)}_{aq}$ -induced recrystallization. More Cr(III) was released during the recrystallization process induced by  $\text{Fe(II)}_{aq}$  at a pH of 7.5, due to the appropriate amount of sorbed Fe(II) onto the surface of goethite. Higher initial  $\text{Fe(II)}_{aq}$  concentrations (>1.0 mM) resulted in the surface passivation of Cr-goethites, and further inhibited Fe atom exchange and Cr(III) release. These findings highlight the important roles of  $\text{Fe(II)}_{aq}$ -induced recrystallization of iron minerals in changing soil metal form and activities, especially in iron-rich environments.

**Author Contributions:** J.H. and M.C. participated in performing the experiments, analyzing the results, and writing the paper; C.L. participated in performing, conceiving, and designing the experiments, as well as in writing and improving the paper; F.L. and J.L. (Jian Long) participated in conceiving the experiments; T.G. participated in analyzing the Fe isotope composition results; F.W. participated in analyzing the Mössbauer spectroscopy results; J.L. (Jing Lei) and M.G. participated in the Cr(III) concentration analysis.

**Funding:** This work was funded by the National Key R&D Program of China (2017YFD0801002), the National Natural Science Foundations of China (U1701241, 41673135 and 41671240), the Science and Technology Foundation of Guangdong Province, China (2016B020242006, 2016A030313780 and 2016TX03Z086), the Science and Technology Foundation of Guangzhou, China (201704020200 and 201710010128), the Innovation Team Program of Modern Agricultural Science and Technology of Guangdong Province (2016LM2149), and the One Hundred Talents Program of the CAS.

**Conflicts of Interest:** The authors declare no conflict of interest.

#### References

- Quantin, C.; Becquer, T.; Rouiller, J.H.; Berthelin, J. Oxide weathering and trace metal release by bacterial reduction in a New Caledonia Ferralsol. *Biogeochemistry* **2001**, *53*, 323–340. [[CrossRef](#)]
- Lu, L.; Wang, R.; Chen, F.; Xue, J.; Zhang, P.; Lu, J. Element mobility during pyrite weathering: implications for acid and heavy metal pollution at mining-impacted sites. *Environ. Geol.* **2005**, *49*, 82–89. [[CrossRef](#)]

3. Cornell, R.M.; Schwertmann, U. *The Iron Oxides: Structure, Properties, Reactions, Occurrences and Uses*, 2nd ed.; Wiley-VCH: Weinheim, Germany, 2003.
4. Trolard, F.; Bourrie, G.; Jeanroy, E.; Herbillon, A.J.; Martin, H. Trace metals in natural iron oxides from laterites: A study using selective kinetic extraction. *Geochim. Cosmochim. Acta* **1995**, *59*, 1285–1297. [[CrossRef](#)]
5. Amstatter, K.; Borch, T.; Larese-Casanova, P.; Kappler, A. Redox transformation of arsenic by Fe(II)-activated goethite ( $\alpha$ -FeOOH). *Environ. Sci. Technol.* **2009**, *44*, 102–108. [[CrossRef](#)] [[PubMed](#)]
6. Hansel, C.M.; Learman, D.R.; Lentini, C.J.; Ekstrom, E.B. Effect of adsorbed and substituted Al on Fe(II)-induced mineralization pathways of ferrihydrite. *Geochim. Cosmochim. Acta* **2011**, *75*, 4653–4666. [[CrossRef](#)]
7. Wells, M.A.; Fitzpatrick, R.W.; Gilkes, R.J. Thermal and mineral properties of Al-, Cr-, Mn-, Ni- and Ti-substituted goethite. *Clay Clay Min.* **2006**, *54*, 176–194. [[CrossRef](#)]
8. Kumpiene, J.; Lagerkvist, A.; Maurice, C. Stabilization of As, Cr, Cu, Pb and Zn in soil using amendments—A review. *Waste Manag.* **2008**, *28*, 215–225. [[CrossRef](#)] [[PubMed](#)]
9. Frierdich, A.J.; Hasenmueller, E.A.; Catalano, J.G. Composition and structure of nanocrystalline Fe and Mn oxide cave deposits: Implications for trace element mobility in karst systems. *Chem. Geol.* **2011**, *284*, 82–96. [[CrossRef](#)]
10. Frierdich, A.J.; Luo, Y.; Catalano, J.G. Trace element cycling through iron oxide minerals during redox-driven dynamic recrystallization. *Geology* **2011**, *39*, 1083–1086. [[CrossRef](#)]
11. Bousserhine, N.; Gasser, U.G.; Jeanroy, E.; Berthelin, J. Bacterial and chemical reductive dissolution of Mn-, Co-, Cr-, and Al-substituted goethites. *Geomicrobiol. J.* **1999**, *16*, 245–258. [[CrossRef](#)]
12. Dominik, P.; Pohl, H.N.; Bousserhine, N.; Berthelin, J.; Kaupenjohann, M. Limitations to the reductive dissolution of Al-substituted goethites by *Clostridium butyricum*. *Soil Biol. Biochem.* **2002**, *34*, 1147–1155. [[CrossRef](#)]
13. Grybos, M.; Davranche, M.; Gruau, G.; Petitjean, P. Is trace metal release in wetland soils controlled by organic matter mobility or Fe-oxyhydroxides reduction? *J. Colloid Interface Sci.* **2007**, *314*, 490–501. [[CrossRef](#)] [[PubMed](#)]
14. Borch, T.; Kretzschmar, R.; Kappler, A.; Cappellen, P.V.; Ginder-Vogel, M.; Voegelin, A.; Campbell, K. Biogeochemical redox processes and their impact on contaminant dynamics. *Environ. Sci. Technol.* **2009**, *44*, 15–23. [[CrossRef](#)] [[PubMed](#)]
15. Kappler, A.; Straub, K.L. Geomicrobiological cycling of iron. *Rev. Mineral. Geochem.* **2005**, *59*, 85–108. [[CrossRef](#)]
16. Williams, A.G.; Scherer, M.M. Spectroscopic evidence for Fe(II)-Fe(III) electron transfer at the iron oxide-water interface. *Environ. Sci. Technol.* **2004**, *38*, 4782–4790. [[CrossRef](#)] [[PubMed](#)]
17. Latta, D.E.; Gorski, C.A.; Scherer, M.M. Influence of Fe<sup>2+</sup>-catalysed iron oxide recrystallization on metal cycling. *Biochem. Soc. Trans.* **2012**, *40*, 1191–1197. [[CrossRef](#)] [[PubMed](#)]
18. Frierdich, A.J.; Catalano, J.G. Controls on Fe(II)-activated trace element release from goethite and hematite. *Environ. Sci. Technol.* **2012**, *46*, 1519–1526. [[CrossRef](#)] [[PubMed](#)]
19. Frierdich, A.J.; Catalano, J.G. Fe(II)-mediated reduction and repartitioning of structurally incorporated Cu, Co, and Mn in iron oxides. *Environ. Sci. Technol.* **2012**, *46*, 11070–11077. [[CrossRef](#)] [[PubMed](#)]
20. Karimian, N.; Johnston, S.G.; Burton, E.D. Antimony and arsenic behavior during Fe(II)-induced transformation of jarosite. *Environ. Sci. Technol.* **2017**, *51*, 4259–4268. [[CrossRef](#)] [[PubMed](#)]
21. Nico, P.S.; Stewart, B.D.; Fendorf, S. Incorporation of oxidized uranium into Fe (hydr)oxides during Fe(II) catalyzed remineralization. *Environ. Sci. Technol.* **2009**, *43*, 7391–7396. [[CrossRef](#)] [[PubMed](#)]
22. Massey, M.S.; Lezama-Pacheco, J.S.; Michel, F.M.; Fendorf, S. Uranium incorporation into aluminum-substituted ferrihydrite during iron(II)-induced transformation. *Environ. Sci.-Process Impacts* **2014**, *16*, 2137–2144. [[CrossRef](#)] [[PubMed](#)]
23. Liu, C.; Zhu, Z.; Li, F.; Liu, T.; Liao, C.; Lee, J.J.; Shih, K.; Tao, L.; Wu, Y. Fe(II)-induced phase transformation of ferrihydrite: The inhibition effects and stabilization of divalent metal cations. *Chem. Geol.* **2016**, *444*, 110–119. [[CrossRef](#)]
24. Jang, J.H.; Dempsey, B.A.; Catchen, G.L.; Burgos, W.D. Effects of Zn(II), Cu(II), Mn(II), Fe(II), NO<sub>3</sub><sup>-</sup>, or SO<sub>4</sub><sup>2-</sup> at pH 6.5 and 8.5 on transformations of hydrous ferric oxide (HFO) as evidenced by Mössbauer spectroscopy. *Colloid Surf. A* **2003**, *221*, 55–68. [[CrossRef](#)]

25. Tchounwou, P.B.; Yedjou, C.G.; Patlolla, A.K.; Sutton, D.J. Heavy metal toxicity and the environment. In *Molecular, Clinical and Environmental Toxicology*; Luch, A., Ed.; Springer: Basel, Switzerland, 2012; Volume 101, pp. 133–164.
26. Zhou, G.; Yin, X.; Zhou, J.; Cheng, W. Speciation and spatial distribution of Cr in chromite ore processing residue site, Yunnan, China. *Acta Geochim.* **2017**, *36*, 291–297. [[CrossRef](#)]
27. Pansar-Kallio, M.; Reinikainen, S.P.; Oksanen, M. Interactions of soil components and their effects on speciation of chromium in soils. *Anal. Chim. Acta* **2001**, *439*, 9–17. [[CrossRef](#)]
28. Singh, B.; Sherman, D.; Mosselmans, J.; Gilkes, R.; Wells, M. Incorporation of Cr, Mn and Ni into goethite ( $\alpha$ -FeOOH): Mechanism from extended X-ray absorption fine structure spectroscopy. *Clay Min.* **2002**, *37*, 639–649. [[CrossRef](#)]
29. Shwertmann, U.; Cornel, R. *Iron Oxides in the Laboratory: Preparation and Characterization*, 3rd ed.; Wiley-VCH: Weinheim, Germany, 2000; pp. 67–92.
30. Notini, L.; Latta, D.E.; Neumann, A.; Pearce, C.I.; Sassi, M.; N'Diaye, A.T.; Rosso, K.M.; Scherer, M.M. The Role of Defects in Fe (II)–Goethite Electron Transfer. *Environ. Sci. Technol.* **2018**, *52*, 2751–2759. [[CrossRef](#)] [[PubMed](#)]
31. Tamura, H.; Goto, K.; Yotsuyanagi, T.; Nagayama, M. Spectrophotometric determination of iron(II) with 1, 10-phenanthroline in the presence of large amounts of iron(III). *Talanta* **1974**, *21*, 314–318. [[CrossRef](#)]
32. Frierdich, A.J.; Helgeson, M.; Liu, C.; Wang, C.; Rosso, K.M.; Scherer, M.M. Iron atom exchange between hematite and aqueous Fe(II). *Environ. Sci. Technol.* **2015**, *49*, 8479–8486. [[CrossRef](#)] [[PubMed](#)]
33. Handler, R.M.; Frierdich, A.J.; Johnson, C.M.; Rosso, K.M.; Beard, B.L.; Wang, C.; Latta, D.E.; Neumann, A.; Pasakarnis, T.; Premaratne, W.A. Fe(II)-catalyzed recrystallization of goethite revisited. *Environ. Sci. Technol.* **2014**, *48*, 11302–11311. [[CrossRef](#)] [[PubMed](#)]
34. Handler, R.M.; Beard, B.L.; Johnson, C.M.; Scherer, M.M. Atom exchange between aqueous Fe(II) and goethite: An Fe Isotope Tracer Study. *Environ. Sci. Technol.* **2009**, *43*, 1102–1107. [[CrossRef](#)] [[PubMed](#)]
35. Sileo, E.; Ramos, A.Y.; Magaz, M.A.; Blesa, M.A. Long-range vs. short-range ordering in synthetic Cr-substituted goethites. *Geochim. Cosmochim. Acta* **2004**, *68*, 3053–3063. [[CrossRef](#)]
36. Tang, Y.Z.; Michel, A.M.; Zhang, L.H.; Harrington, R.; Parise, J.B.; Reeder, R.J. Structural properties of the Cr(III)-Fe(III) (oxy)hydroxide compositional series: Insights for a nanomaterial “solid solution”. *Chem. Mater.* **2012**, *22*, 3589–3598. [[CrossRef](#)]
37. Latta, D.E.; Bachman, J.E.; Scherer, M.M. Fe electron transfer and atom exchange in goethite: Influence of Al-substitution and anion sorption. *Environ. Sci. Technol.* **2012**, *46*, 10614–10623. [[CrossRef](#)] [[PubMed](#)]
38. Cwiertny, D.M.; Handler, R.M.; Schaefer, M.V.; Grassian, V.H.; Scherer, M.M. Interpreting nanoscale size-effects in aggregated Fe-oxide suspensions: Reaction of Fe(II) with goethite. *Geochim. Cosmochim. Acta* **2008**, *72*, 1365–1380. [[CrossRef](#)]
39. Kaneko, K.; Inoue, N.; Ishikawa, T. Electrical and photoadsorptive properties of valence-controlled  $\alpha$ -FeOOH. *J. Phys. Chem.* **1989**, *93*, 1988–1992. [[CrossRef](#)]
40. Rai, D.; Sass, B.M.; Moore, D.A. Chromium(III) hydrolysis constants and solubility of chromium(III) hydroxide. *Inorg. Chem.* **1987**, *26*, 345–349. [[CrossRef](#)]
41. Klyukin, K.; Rosso, K.M.; Alexandrov, V. Iron dissolution from goethite ( $\alpha$ -FeOOH) surfaces in water by ab initio enhanced free-energy simulations. *J. Phys. Chem. C* **2018**, *122*, 16086–16091. [[CrossRef](#)]
42. Kosmulski, M. *Chemical Properties of Material Surfaces*; CRC Press: New York, NY, USA, 2001.
43. Pedersen, H.D.; Postma, D.; Jakobsen, R.; Larsen, O. Fast transformation of iron oxyhydroxides by the catalytic action of aqueous Fe(II). *Geochim. Cosmochim. Acta* **2005**, *69*, 3967–3977. [[CrossRef](#)]
44. Reddy, T.R.; Frierdich, A.J.; Beard, B.L.; Johnson, C.M. The effect of pH on stable iron isotope exchange and fractionation between aqueous Fe(II) and goethite. *Chem. Geol.* **2015**, *397*, 118–127. [[CrossRef](#)]
45. Joshi, P.; Gorski, C.A. Anisotropic morphological changes in goethite during Fe<sup>2+</sup>-catalyzed recrystallization. *Environ. Sci. Technol.* **2016**, *50*, 7315–7324. [[CrossRef](#)] [[PubMed](#)]
46. Rosso, K.M.; Yanina, S.V.; Gorski, C.A.; Laresecanova, P.; Scherer, M.M. Connecting observations of hematite ( $\alpha$ -Fe<sub>2</sub>O<sub>3</sub>) growth catalyzed by Fe(II). *Environ. Sci. Technol.* **2010**, *44*, 61–67. [[CrossRef](#)] [[PubMed](#)]
47. Yanina, S.V.; Rosso, K.M. Linked reactivity at mineral-water interfaces through bulk crystal conduction. *Science* **2008**, *320*, 218–222. [[CrossRef](#)] [[PubMed](#)]
48. Larese-Casanova, P.; Scherer, M.M. Fe(II) sorption on hematite: New insights based on spectroscopic measurements. *Environ. Sci. Technol.* **2007**, *41*, 471–477. [[CrossRef](#)] [[PubMed](#)]

49. Frierdich, A.J.; Scherer, M.M.; Bachman, J.E.; Engelhard, M.H.; Rapponotti, B.W.; Catalano, J.G. Inhibition of trace element release during Fe(II)-activated recrystallization of Al-, Cr-, and Sn-substituted goethite and hematite. *Environ. Sci. Technol.* **2012**, *46*, 10031–10039. [[CrossRef](#)] [[PubMed](#)]
50. Zarzycki, P.; Kerisit, S.; Rosso, K.M. Molecular dynamics study of Fe(II) adsorption, electron exchange and mobility at goethite ( $\alpha$ -FeOOH) surfaces. *J. Phys. Chem. C* **2015**, *119*, 3111–3123. [[CrossRef](#)]



© 2018 by the authors. Licensee MDPI, Basel, Switzerland. This article is an open access article distributed under the terms and conditions of the Creative Commons Attribution (CC BY) license (<http://creativecommons.org/licenses/by/4.0/>).